Cerebral Cortex, December 2019; 5217–5233

doi: 10.1093/cercor/bhz060
Advance Access Publication Date: 7 April 2019
Original Article

ORIGINAL ARTICLE

Altered Cortical Brain Structure and Increased Risk for Disease Seen Decades After Perinatal Exposure to Maternal Smoking: A Study of 9000 Adults in the UK Biobank

Lauren E. Salminen[1], Rand R. Wilcox[2], Alyssa H. Zhu[1], Brandalyn C. Riedel[1,3], Christopher R. K. Ching[1], Faisal Rashid[1], Sophia I. Thomopoulos[1], Arvin Saremi[1], Marc B. Harrison[1], Anjanibhargavi Ragothaman[1], Victoria Knight[1], Christina P. Boyle[1], Sarah E. Medland[4], Paul M. Thompson[1] and Neda Jahanshad[1]

[1]Imaging Genetics Center, USC Mark and Mary Stevens Neuroimaging and Informatics Institute, Keck School of Medicine of the University of Southern California, Marina del Rey, CA 90292 USA, [2]Department of Psychology, University of Southern California, Los Angeles, CA 90089-1061, USA, [3]Department of Radiology and Imaging Sciences, Indiana University School of Medicine, Indianapolis, IN, USA and [4]QIMR Berghofer Medical Research Institute, Brisbane 4006, Australia

Address correspondence to Lauren E. Salminen, PhD, Imaging Genetics Center, USC Mark and Mary Stevens Neuroimaging and Informatics Institute, Keck School of Medicine of the University of Southern California, Marina del Rey, CA, 90292 USA. Email: lauren.salminen@loni.usc.edu

Abstract

Secondhand smoke exposure is a major public health risk that is especially harmful to the developing brain, but it is unclear if early exposure affects brain structure during middle age and older adulthood. Here we analyzed brain MRI data from the UK Biobank in a population-based sample of individuals (ages 44–80) who were exposed ($n = 2510$) or unexposed ($n = 6079$) to smoking around birth. We used robust statistical models, including quantile regressions, to test the effect of perinatal smoke exposure (PSE) on cortical surface area (SA), thickness, and subcortical volumes. We hypothesized that PSE would be associated with cortical disruption in primary sensory areas compared to unexposed (PSE^-) adults. After adjusting for multiple comparisons, SA was significantly lower in the pericalcarine (PCAL), inferior parietal (IPL), and regions of the temporal and frontal cortex of PSE^+ adults; these abnormalities were associated with increased risk for several diseases, including circulatory and endocrine conditions. Sensitivity analyses conducted in a hold-out group of healthy participants (exposed, $n = 109$, unexposed, $n = 315$) replicated the effect of PSE on SA in the PCAL and IPL. Collectively our results show a negative, long term effect of PSE on sensory cortices that may increase risk for disease later in life.

Key words: aging, perinatal smoke exposure, secondhand smoke, structural neuroimaging, UK Biobank

Introduction

Tobacco use is a major public health concern worldwide. According to the World Health Organization (WHO), there are currently 1.1 billion daily smokers globally, exposing more than one-third of the adult world population to secondhand smoke. Global smoking trends show a recent net decline in smoking prevalence, but this is primarily driven by decreased smoking prevalence in high income countries. Further, the total number of smokers worldwide has not fallen overall due to population growth, particularly in low- and middle-income countries (LMICs) that account for 80% of the world's daily smokers (WHO 2018). Tobacco smoke is currently responsible for 6 million deaths annually, including 600,000 deaths from secondhand smoke. If current trends persist, around half of current smokers will die prematurely from tobacco use by 2050, with a disproportionate hit to LMICs (WHO 2018).

Health risks associated with cigarette smoke can be traced to more than 7000 chemical compounds, including over 4500 toxins and approximately 70 carcinogens (Choi et al. 2017) Approximately 15% of cigarette smoke is ingested by the smoker, while the remainder is released into the atmosphere. Cigarette smoke is more harmful to children, infants, and the developing fetus than to adults due to their faster respiratory rates that result in greater smoke consumption. Their underdeveloped lungs and immune systems further increase the risk for acute and chronic illnesses (CDC 2018). Accordingly, exposure to maternal smoking and environmental tobacco smoke increases risk for spontaneous preterm abortion, poor intrauterine lung function, low birthweight in neonates (Hofhuis et al. 2003), Sudden Infant Death Syndrome (SIDS), middle ear disease, asthma and respiratory disease, vision problems, neurodevelopmental conditions in children, cardiovascular disease, and psychiatric illness (Polanska et al. 2008; Blood-Siegfried and Rende 2010; CDC 2017). There is also increasing evidence that perinatal smoke exposure (PSE) influences structural brain development (Toro et al. 2008; Derauf et al. 2012; Liu et al. 2013; El Marroun et al. 2014), which may impair physical and mental health later in life.

Nicotine is the most widely studied constituent of tobacco smoke due to its addictive properties and ability to enter the brain within seconds of consumption (Berridge et al. 2010). In the brain, nicotine alters the activity of nicotinic acetylcholine receptors (nAChRs), which play an important role in neuronal maturation when bound by the neurotransmitter, acetylcholine (ACh). The pharmacological action of nAChRs is determined by homomeric and heteromeric complexes of α and β protein subunits that are widely distributed throughout the brain (Gotti et al. 2006). Localized expression of nAChR subunit configurations facilitates distinct functions during early brain development, including (but not limited to) neuronal pathfinding, the formation of essential neural circuits and sensory structures (Bansal et al. 2000) and regulation of brain stem networks (O'Leary et al. 2008). In the early postnatal period, the functional patterns of nAChRs are critical for regulating synaptic pruning in the neocortex (Orr-Urtreger et al. 2000), thalamocortical synaptic maturation, and sensory signaling (Metherate and Hsieh 2003; Aztiria et al. 2004). Accordingly, dysregulated nAChR activity in animal studies and wet lab work has been linked to attenuated neuronal differentiation, apoptosis, desensitized synaptic circuits, and lower cell density in the somatosensory cortex (Slotkin 2004; Chatterton et al. 2017). Other work (Swan and Lessov-Schlaggar 2007; Coggins et al. 2013; Singh et al. 2017) suggests there is a multi-mechanistic role of nicotine and other harmful cigarette compounds on brain structure, but human research in this area is limited relative to articles on the bioactive effects of nicotine.

Most tobacco-related morbidities occur decades after initial tobacco use and secondhand smoke exposure (Holford et al. 2014). Thus, today's current population of middle-aged individuals (ages 40–65) is the highest risk group for tobacco-related illness and early death. This mortality risk includes nonsmokers exposed to secondhand smoke, with disproportionately higher risk among those exposed at younger ages (Diver et al. 2018). PSE has been identified as a long-term risk for cancer, cardiovascular disease, and other systemic morbidities (CDC 2017), but we lack understanding of the long-term effects of PSE on brain structure in middle and old age, and how this altered brain structure may further relate to risk for health conditions. Given the known biological repercussions of tobacco smoke and delayed onset of smoke-attributable disease, identifying the long-term effects of PSE on brain structure may be used to inform tobacco control policies and public health warnings for smoking prevention and cessation (WHO 2018).

The UK Biobank (UKB) is currently the largest-ever prospective study of aging, collecting detailed health, physical, and lifestyle information for 500,000 middle aged and older adults living in the United Kingdom (UK). Here we analyzed available magnetic resonance imaging (MRI) data from the UKB to examine cortical and subcortical brain structure in a subset of PSE^+ and PSE^- (unexposed) individuals who completed neuroimaging. Based on earlier work (Toro et al. 2008; Derauf et al. 2012; Liu et al. 2013; El Marroun et al. 2014), we hypothesized that cortical measurements would be preferentially associated with PSE relative to subcortical gray matter indices, with the most robust effects in surface area (SA) of primary sensory cortices—regions that mature rapidly during the neonatal period.

Methods

Participants

Data were analyzed from a population-based sample of individuals from the UKB (Application ID#11559; July 2017 release) who completed neuroimaging (N = 8589; males, n = 4050, females, n = 4539; M_{age} = 62.5, SD = 7.5), and a separate group of participants without any self-reported or medically documented health conditions (herein referred to as "elite healthy" (N = 424; males, n = 218, females, n = 206; M_{age} = 59.7, SD = 7.2; Table 1). The impetus to examine elite healthy individuals separate from the full sample was to better isolate effects of PSE by eliminating individuals with conditions that might directly or indirectly impact brain structure. All participants were between the ages of 44 and 80 years. Exclusion criteria for the whole sample were limited to safety factors that precluded neuroimaging (e.g., metal implants, recent surgery, etc.). Individuals in the elite healthy sample were excluded for any documented health condition identified through self-report or hospital records indexing medical diagnoses via the 10th revision of the International Classification of Diseases (ICD-10), and contraindications for MRI. All participants provided informed consent prior to study participation. Data analyzed in this manuscript are publicly available through approved research applications submitted to UKB (http://www.ukbiobank.ac.uk/register-apply/).

Neuroimaging Acquisition

Participants completed a 31-minute neuroimaging protocol at the UKB imaging center in Cheadle, Manchester, UK. All scans

Table 1 Descriptive Characteristics of the Samples

Descriptive variables	Population-based sample N = 8589		Elite healthy replication sample N = 424	
	PSE$^-$	PSE$^+$	PSE$^-$	PSE$^+$
Age, M(SD)	62.7(7.6)**	62.2(7.1)**	59.6(7.4)	59.9(6.4)
Waist/hip ratio, M(SD)	0.86(0.08)***	0.87(0.08)***	0.85(0.8)	0.84(0.8)
Townsend Index, M(SD)	2.0(2.6)***	1.8(2.7)***	2.1(2.5)	2.3(2.5)
Sex, % Male	47.3%***	46.7%***	47.3%***	52.3%***
Education, % College	68.3%***	64.1%***	76%***	64%***
Adult Smoker, % Yes	37.8%***	35.1%***	29.5%	30.3%
ICD-10 Conditions by ICD Chapter [a], % Yes:				
Infections/parasitic disease (A00-B99)	4.7%	5.4%	–	–
Neoplasms (C00-D49)	17.9%	18.4%	–	–
Blood (D50-D89)	3.8%	4.2%	–	–
Endocrine (E00-E89)	12.0%	12.7%	–	–
Psychiatric (F01-F99)	3.8%**	5.4%**	–	–
CNS (G00-G99)	5.9%*	7.3%*	–	–
Eye (H00-H59)	7.9%	7.8%	–	–
Ear (H60-H95)	1.5%	2.0%	–	–
Circulatory (I00-I99)	23.8%**	26.4%**	–	–
Respiratory (J00-J99)	10.6%*	12.3%*	–	–
Digestive (K00-K95)	32.6%**	36.0%**	–	–
Skin (L00-L99)	9.2%	8.4%	–	–
Musculoskeletal (M00-M99)	18.7%*	20.6%*	–	–
Genitourinary (N00-N99)	22.8%**	25.6%**	–	–
Pregnancy-related (O00-O9A)	4.3%	4.1%	–	–
Congenital (Q00-Q99)	0.8%	1.1%	–	–

Note: Demographic numbers vary slightly per analysis. [a]Not reported are conditions originating in the perinatal period, as there was only one subject in our sample with an ICD-10 diagnosis in this category. We also did not include ICD-10 codes after Q99, as these ICD categories are heterogeneous and challenging to interpret in relation to brain metrics. ***$P < 0.001$, **$P < 0.01$, *$P < 0.05$.

were conducted on a single Siemens Skyra 3 tesla scanner, running software VD13A-SP4 with a 32-channel radiofrequency receiver head coil. Structural T1-weighted brain scans were acquired using the following parameters: 3D magnetization prepared rapid acquisition gradient-echo (MPRAGE), sagittal orientation, in-plane acceleration factor = 2, resolution = 1.0 × 1.0 × 1.0 mm^3 voxels, TI/TR = 800/2000 ms. Scans were pre-scan normalized using an on-scanner bias-field correction filter. The scanning protocol is further detailed in Miller et al. (2016) and Alfaro-Almagro et al. (2018).

Image Processing

At the time of the July 2017 data release and analysis, cortical surface area (SA) and thickness (CT) were not available from the UKB data showcase. We therefore, independently extracted CT and SA values using the image processing software, FreeSurfer, version 5.3 (Fischl 2012), and the cortical extraction and quality control (QC) protocols we developed for the Enhancing Neuro Imaging Genetics through Meta-Analyses (ENIGMA) consortium (http://enigma.usc.edu/protocols/imaging-protocols/). The extraction protocol yields CT and SA values for 68 cortical regions of interest (ROIs) across the left and right hemispheres according to the Desikan-Killiany atlas (Desikan et al. 2006). FreeSurfer segmentations underwent a rigorous QC procedure, detailed on the ENIGMA website. Participants with scans that failed the visual QC entirely, due to either anatomical abnormalities or scan artifacts, were excluded. Out of 10573 scans, 171 failed the visual QC entirely and were unusable. Of the remaining scans, 3412 exhibited minor segmentation errors in which values for discrete regions were removed prior to statistical analysis. As we did not hypothesize any lateralized effects of PSE, measures from bilateral ROIs were averaged across hemispheres for data reduction.

We used the imaging-derived phenotypes released by UKB to examine subcortical volumes (VOL) for the thalamus, pallidum, putamen, caudate, amygdala, hippocampus, and nucleus accumbens, which were also averaged across both hemispheres. Subcortical VOLs were computed using *FMRIB's Integrated Registration and Segmentation Tool* (FIRST) from the FMRIB Software Library (FSL; Patenaude et al. 2011).

Operational Definitions of Predictor Variables

Perinatal Smoke Exposure

Perinatal smoke exposure (PSE) was assessed from a touchscreen questionnaire on early life factors. Participants were asked, "Did your mother smoke regularly around the time when you were born?" (data field 1787, http://biobank.ctsu.ox.ac.uk/crystal/field.cgi?id = 1787). Responses were recorded as "yes" ($n = 2663$), "no" ($n = 6502$), "do not know" ($n = 552$), or "prefer not to answer" ($n = 1$). Here we analyzed "yes" (exposed to PSE) and "no" (unexposed to PSE) responses.

Sociodemographic Factors

Proxy measures for sociodemographic factors were examined across levels of the PSE grouping variable to identify potential confounders of brain structure that are salient in PSE$^+$ populations. The following variables were examined in addition to age and sex:

- *Educational attainment* was assessed using a sociodemographic questionnaire in which participants reported their completed

qualification levels according to the UK education system (data field 6138). Possible responses included[1] "College or University Degree", "A levels/AS levels or equivalent", "O levels/GCSEs or equivalent", "CSEs or equivalent", "NVQ or HND or HNC or equivalent", "Other professional qualification", "None of the above", or "Prefer not to answer". To generalize results beyond the UK education system, we converted each response to the corresponding "number of years" using harmonization guidelines from the International Standard Classification of Education (ISCED; Goujon et al. 2016). Closer examination of these variables revealed a relatively small sample space for years of education, which functioned as a discrete variable in our dataset. To improve the stability of our statistical models, we dichotomized education into "college" versus "no college (high school or less)" education groups based on the maximum number of completed education levels (college ≥17 years in the UK education system).

- *Socioeconomic status* (SES) was measured using the Townsend Index (Townsend et al. 1988) (data field 189)—a measure of societal deprivation—based on the postal code of the participant. Townsend scores are widely used as a proxy measure of SES (Smith et al. 2001); prior work in this sample shows high genetic correlations between Townsend scores, psychiatric conditions, and diseases of the central nervous system, as well as specific biomarkers of physical health (Hill et al. 2016). Townsend scores were multiplied by (−1) so that higher scores indicated higher SES.
- *Population structure* was assessed using 4 principal components from the multidimensional scaling protocol of the UKB genetic ancestry analysis. In subsequent text and figures, these are denoted C1, C2, C3, and, C4.

Adult Smoking

We examined potential intervening effects of adulthood smoking on brain measures using the variable "Smoking status" (data field 20116), for which responses included "never smoked" (n = 5670), "previous smoker" (n = 3116), "current smoker" (n = 362), or "prefer not to answer" (n = 17). To reduce the number of comparisons, we collapsed previous and current smokers into one group and contrasted them against "never smokers" and levels of the PSE grouping variable.

Waist-to-Hip Ratio

We analyzed waist-to-hip ratio (WHR) (data fields 48–49) to index potential differences in physical/cardiovascular health between PSE groups. WHR is a common index of central fat distribution that has been linked to PSE (Santos et al. 2016). Prior work shows a strong positive correlation between WHR and visceral fat in healthy adults (Gadekar et al. 2018). WHR is also a marker of atherosclerotic burden in overweight individuals and postmenopausal women (Lee et al. 2015; Scicali et al. 2018), and a risk factor for major cardiovascular events and death in women with heart disease (Medina-Inojosa et al. 2018; Streng et al. 2018), and mortality in men (Mousavi et al. 2015). Waist and hip measurements were obtained manually at the time of the imaging scan.

Birth Weight

Birth weight was reported retrospectively in 5915 participants of the population-based sample and 292 participants in the elite healthy sample. Maternal smoking during pregnancy is consistently linked to low birthweight in neonates if smoking behaviors continue beyond the first trimester (Ding et al. 2017). Thus, we analyzed whether observed effects between PSE and brain structure would persist after covarying for differences in birth weight—an indicator of prenatal health (Gortmaker 1979; Kogan et al. 1994; Alexander and Korenbrot 1995). Birth weight was reported in kg units.

Analytic Approach

Chi-squared analyses and independent samples t-tests were run to describe potential differences in sociodemographics, adult smoking behavior, and WHR between PSE^+ (perinatally exposed) and PSE^- (unexposed) groups. These variables served as covariates in the main analyses and did not indicate problematic multicollinearity indexed with the variance inflation factor. Continuous covariates and dependent variables were z-transformed prior to analysis to standardize results and facilitate interpretation. We also performed chi-squared tests between PSE and binary ICD-10 codes to better characterize the population-based sample. As the cell sizes for many conditions were limited, we aggregated individual disease codes into ICD-10-chapter codes using the ICD classification system (https://www.icd10data.com/ICD10CM/Codes).

For the primary analyses, we computed 3 series of ordinary least squares (OLS) linear regression models to determine whether brain structure differed between $PSE^{+/-}$ groups using imaging metrics of (1) cortical thickness (CT), (2) cortical surface area (SA), and (3) subcortical volumes (VOL). Age and sex were included as covariates in all models, and intracranial volume (ICV) was included as a covariate in SA and VOL regressions. False discovery rate (FDR) corrections were applied to correct for multiple comparisons across the 75 brain metrics (34 CT metrics, 34 SA metrics, 7 VOL metrics) using the Benjamini-Hochberg method (Benjamini and Hochberg 1995). Regression models were then re-analyzed using the same approach as the main analysis after including birth weight as a covariate predictor. We did not covary for birth weight in the main analysis to avoid regressing out the effects of PSE and/or conflating them with other prenatal factors (stress, nutrition, etc.).

Sensitivity analyses were completed in the elite healthy sample (PSE^+, n = 109; PSE^-, n = 315) for brain regions that differed significantly by PSE, using the same statistical analyses used in the population-based sample. These participants were held out of our main analysis for replication.

Preliminary Analyses

Neuroimaging variables were checked for normality and homoscedasticity at the model level using Kolmogorov–Smirnov (Massey 1952) and Koenker–Bassett tests (Koenker and Bassett 1982). Outliers and leverage points among the covariates were checked using robust projection methods originally described by Wilcox and Keselman (2012), and later adapted with the Wilcox Robust Statistical package (WRS2) in R (Mair and Wilcox

[1]A levels = Advanced level subject-based qualification as part of the General Certificate of Secondary Education (GCSE); O levels/GCSEs = Ordinary Level GCSE; CSE = Certificate of Secondary Education; NVQ = National Vocational Qualification; HND = Higher National Diploma; HNC = Higher National Certificate.

2016). Examination of the data indicated there was heteroscedasticity. That is, the variation in the neuroimaging variables depended on the values of the independent variables. Additionally, the data were not normal. We used 2 methods to combat these issues. First, we applied an HC4 standard error estimator to the OLS models using the "olshc4" function in R. The HC4 method (Cribari-Neto 2004) deals with heteroscedasticity data but is highly conservative, with a null rejection rate at ~1% (Cribari-Neto et al., 2014). Moreover, OLS can be negatively impacted by outliers. Thus, we computed quantile regressions in addition to OLS models to show how different results can be derived using robust statistical methods that appropriately account for the impact of skewness. To do this, we used the "regci" function in R (Wilcox and Keselman 2012) with a quantile regression estimator. We tested the hypothesis that predictor slopes, particularly from the PSE grouping variable, were *not* equal to zero using the (conditional) quantiles = 0.1, 0.25, 0.5, 0.75, 0.9 associated with the dependent variable. We applied a separate FDR correction threshold for the 75 metrics at each quantile (375 comparisons).

Estimating Effect Size

We used multiple methods for evaluating effect size in both OLS and quantile regression models. For both types of models, z-transformation of continuous independent and dependent variables allowed us to compute scaled beta weights for each individual predictor. These estimates of effect size are shown in Figures 1–3 and reflect the individual effect size of each predictor as a function of the multivariate model. Model-specific effect size estimates are described briefly below (See Appendix for detail).

Effect Sizes for OLS Regressions

We used least angle regression LASSO to sort multivariate predictors in order of importance based on the beta weights, standard errors, and confidence intervals of each variable (Figs 1 and 3). Thus, the effect sizes of each predictor can be interpreted using individual beta weights and by relative rank in the model. For group comparisons, we computed robust analogs of Cohen's *d* (Algina et al. 2005) using 20% trimmed means and Winsorized standard deviations. Previous work, including theory and simulation studies (Wilcox 1995c, 1996), show that a 20% trimmed mean is a good solution for dealing with outliers and skewed distributions because it achieves more accurate confidence intervals and a small standard error (Wilcox and Serang 2017; see Appendix for more detail). However, robust estimations become complicated when the predictor set includes discrete variables. As such, robust effect size estimates in this study only account for the strength of association between *x* (PSE) and *y* (ROI). The magnitude of effect size can be interpreted using absolute values of Cohen's guidelines: 0.2 (small), 0.5 (medium), and 0.8 (large).

Effect sizes for quantile regressions

To add perspective, effect sizes were computed for brain metrics that differed by PSE using the quantile shift function in R (Wilcox, in press). Briefly, when groups do not differ, the median of the typical difference, *x*–*y*, is zero. A quantile shift effect size (QS) reflects a shift of the median to a higher or

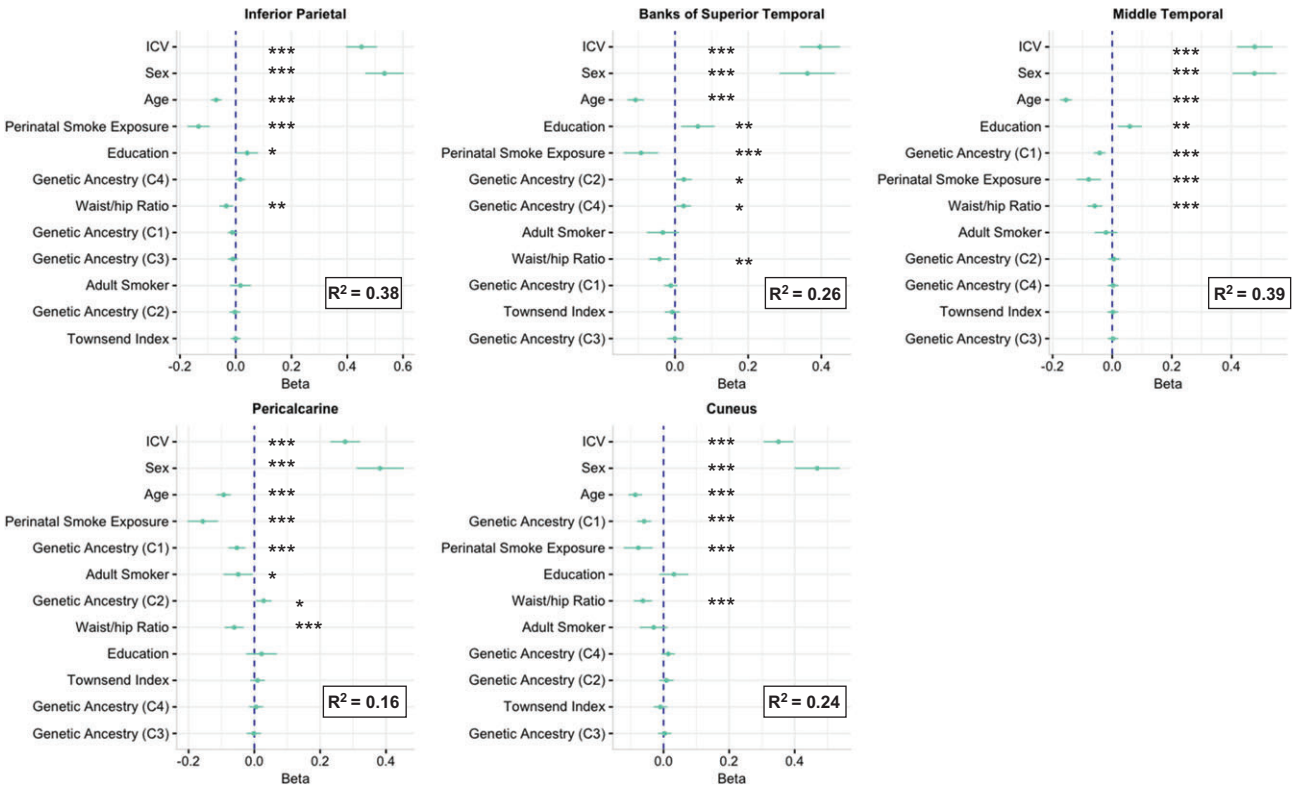

Figure 1. Beta weights for cortical surface area regions that differed by PSE in the population-based sample. Predictor variables are plotted on the y axis in order of importance using least angle regression LASSO. The individual principle components of genetic ancestry are indicated in parentheses. ***P < 0.001, **P < 0.01, *P < 0.05.

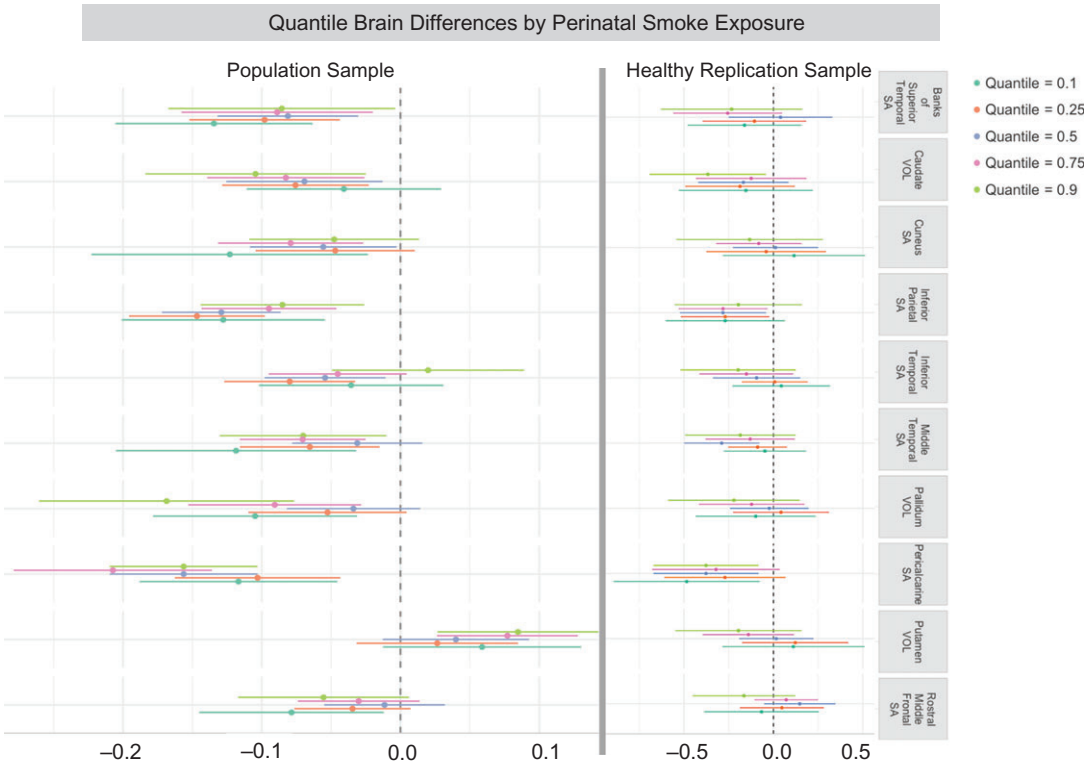

Figure 2. Beta weights of neuroimaging metrics that differed significantly by PSE. Dot-whisker plots on the left depict beta weights of observed brain differences in the population-based sample. Plots on the right reflect the replication results in the healthy sample. SA = surface area, VOL = volume.

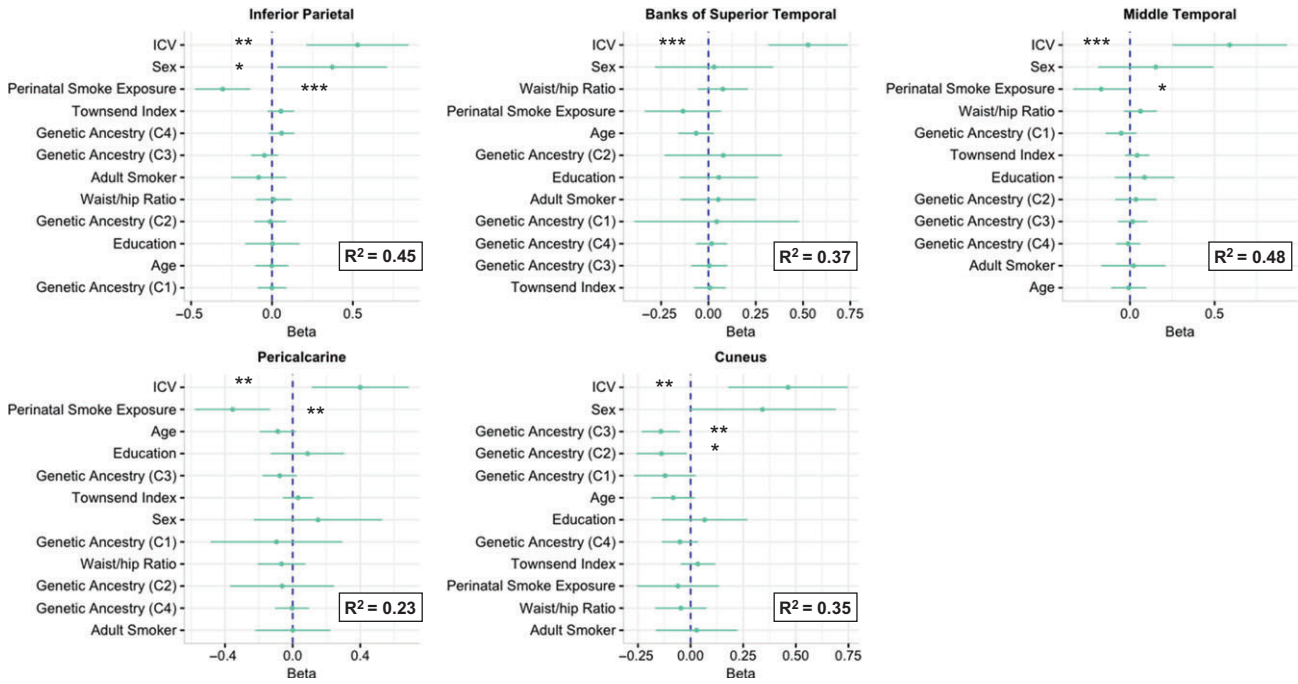

Figure 3. Beta weights of predictors in the healthy replication sample. Predictor variables are plotted on the y axis in order of importance for each model using least angle regression LASSO. The individual principle components of genetic ancestry are indicated in parentheses. PSE was not a significant predictor of surface area in the banks of superior temporal sulcus or cuneus. ***P < 0.001, **P < 0.01, *P < 0.05.

lower quantile associated with the distribution of x–y; it deals with non-normality and does not assume homoscedasticity. Under normality and homoscedasticity, Cohen's d = 0, 0.2, 0.5, and 0.8 corresponds approximately to a QS effect of 0.5, 0.55, 0.65, and 0.7, respectively (Wilcox, in press).

Brain Structural Contributions to PSE-Related Disease Risk

To determine the clinical relevance of the significant models observed in our study, we completed *post hoc* logistic regressions to determine relative risk of developing specific classes of ICD-10 medical conditions (e.g., psychiatric). We used a Partial *F*-test to determine whether region-specific brain structure significantly contributed to explaining the population variance. "Partial models" were computed to determine relative risk for each ICD-10 condition class using the independent variables in our main analysis. "Full models" were then computed by adding neuroimaging variables that differed significantly by PSE in the main analysis to each predictor set. These models were first conducted in the whole sample to determine the relative risk ratio (RR) of PSE, and then conducted within PSE groups. These analyses were completed in a reduced sample that removed all listwise missingness ($PSE^+ = 1945$; $PSE^- = 4784$). Significance for these analyses was determined at a threshold of $P < 0.05$, as these were *post hoc* analyses and included regions and disorders already determined to be significant after FDR correction; further correcting for multiple comparisons also may have a greater public health risk of a type 2 error. We did not include birth weight as a predictor in these analyses given the lower number of participants who provided this information ($N = 5915$, further reduced when accounting for each disease), and its inherent association to PSE. However, we did use ICV as a predictor in these models, as smaller head size is a reported outcome of prenatal smoking and early environmental tobacco smoke exposure (Bouthoorn et al. 2012). We did not examine ICD-10 classes of "Symptoms not otherwise specified" (ICD codes R00-R99), "Consequences of external causes" (S00-T88), "External causes of morbidity" (V00-Y99), or "Factors influencing health status" (Z00-Z99) given the heterogeneous nature of these ICD categories.

All analyses were conducted using two-tailed tests in R. A detailed description of the OLS and quantile regression approach and corresponding code is included in the Appendix.

Results

Cohort Demographics and Comparisons of Descriptive Variables

Sociodemographic characteristics of the sample are provided in Table 1. The sample size varied per analysis due to differences in data availability across imaging metrics, ROIs that failed the cortical QC, and presence of outliers. Participants in the PSE^+ group were significantly younger ($t(8587) = 2.7$, $P = 0.006$), had a higher WHR ($t(8578) = -3.5$, $P < 0.001$), lower education ($t(8582) = 5.11$, $P < 0.001$), and lower SES indicated by their Townsend scores ($t(8583) = 3.6$, $P < 0.001$). Chi-squared analysis showed that a greater proportion of the PSE^- (unexposed) group was male ($\chi^2(1) = 584.1$, $P < 0.001$) and a past or current smoker ($\chi^2(1) = 156.7$, $P < 0.001$) when compared to the PSE^+ group. Chi-squared analysis also showed that a lower proportion of the PSE^+ group had completed any years of college when compared to the PSE^- group ($\chi^2(1) = 13.9$, $P < 0.001$). Analysis of ICD-10 conditions showed that a greater proportion of the PSE^+ group was diagnosed with the following classes of disease: psychiatric ($\chi^2(1) = 11.6$, $P < 0.001$), central nervous system ($\chi^2(1) = 5.77$, $P = 0.016$), circulatory ($\chi^2(1) = 6.79$, $P = 0.009$), respiratory ($\chi^2(1) = 5.69$, $P = 0.017$), digestive ($\chi^2(1) = 8.97$, $P = 0.003$), musculoskeletal ($\chi^2(1) = 4.15$, $P = 0.042$), and genitourinary conditions ($\chi^2(1) = 7.42$, $P = 0.006$).

PSE groups within the elite healthy replication sample did not differ significantly on age ($t(422) = -0.26$, $P = 0.794$), WHR ($t(422) = 0.78$, $P = 0.433$) or Townsend scores ($t(421) = -0.44$, $P = 0.657$). Chi-squared tests showed that a smaller proportion of the PSE^+ group was male ($\chi^2(1) = 58.1$, $P < 0.001$) and had a college-level education ($\chi^2(1) = 187.9$, $P < 0.001$). There were no significant group differences in adult smoking ($\chi^2(1) = 1.7$, $P = 0.229$).

Brain Structural Differences by PSE

Using OLS regression with an HC4 estimator, individuals in the PSE^+ group demonstrated significantly lower SA in the pericalcarine (PCAL; $n = 7159$; $\beta = -0.16$, 95% CIs[−0.20,−0.11], $P = 5.0 * 10^{-11}$), inferior parietal cortex (IPL; $n = 7634$; $\beta = -0.13$, 95% CIs [−0.17,−0.09], $P = 6.8 * 10^{-11}$), banks of the superior temporal sulcus (bSTS; $n = 6660$; $\beta = -0.09$, 95% CIs[−0.14,−0.05], $P = 1.2 * 10^{-4}$), middle temporal gyrus (MTG; $n = 7225$; $\beta = -0.08$, 95% CIs [−0.12,−0.04], $P = 1.4 * 10^{-4}$), and cuneus (CUN, $n = 7235$; $\beta = -0.08$, 95% CIs[−0.12,−0.03], $P = 6.8 * 10^{-4}$). Groups did not differ significantly on metrics of CT or VOL. Examination of covariate effects on SA revealed positive associations with sex and ICV, and negative associations with age and WHR in each of these regions. Education was positively associated with SA in all regions except the PCAL (Fig. 1). As detailed in Figure 4, effect sizes for brain differences by PSE were small, ranging from 0.08 (CUN) to 0.18 (PCAL).

Quantile regressions revealed similar findings in some regions, but different effects in others. Specifically, individuals in the PSE^+ group showed significantly lower SA in the PCAL and IPL at quantiles 0.1–0.75, the bSTS at quantiles 0.1–0.5, the MTG at quantiles 0.1–0.25 and 0.75–0.9, and the ITG at quantile 0.25 (Fig. 2*a*). Trend effects ($p < 0.01$) were observed for lower SA in the CUN and RMFG at quantile 0.75, and lower VOL in the caudate, pallidum, and putamen at quantile 0.75. The pallidum also trended towards significance at the 0.9 quantile (Supplementary Table 1). SA and VOL in these regions were negatively associated with age, and positively associated with sex and ICV at all quantiles of the regressions. After age, sex, and ICV, the 2 most common predictors of SA were WHR and the first multidimensional scaling component of genetic ancestry (C1). WHR was also negatively associated with VOL in the caudate, pallidum, and putamen, but associations varied across quantiles. Finally, college education was positively associated with VOL in the caudate, pallidum, and putamen, but associations were only observed at lower quantiles ($q = 0.1$–0.5). Quantile shift effect sizes were small in all regions that differed significantly by PSE or trended towards significance (Table 2*a*).

After covarying for birth weight, the PSE^+ group demonstrated significantly lower SA in the PCAL and IPL in all quantiles. Effects were strongest for the 0.25 and 0.5 quantiles for the IPL (β's = −0.1 and −0.12, respectively), and the 0.25–0.75 quantiles for the PCAL. Birth weight was positively associated with SA in the IPL for all quantiles (Supplementary Table 1). We did not detect significant associations between birth weight and SA in the PCAL at any point along the distribution (Supplementary Table 2).

Replication in the Elite Healthy Sample

Replication analyses using the OLS approach revealed lower SA in the PCAL ($n = 354$; $\beta = -0.36$, 95% CIs[−0.53, −0.07], $P = 0.009$), IPL ($n = 362$; $\beta = -0.32$, 95% CIs[−0.49, −0.14], $P < 0.001$), and MTG ($n = 341$; $\beta = -0.19$, 95% CIs[−0.36, −0.02], $P = 0.028$) of the

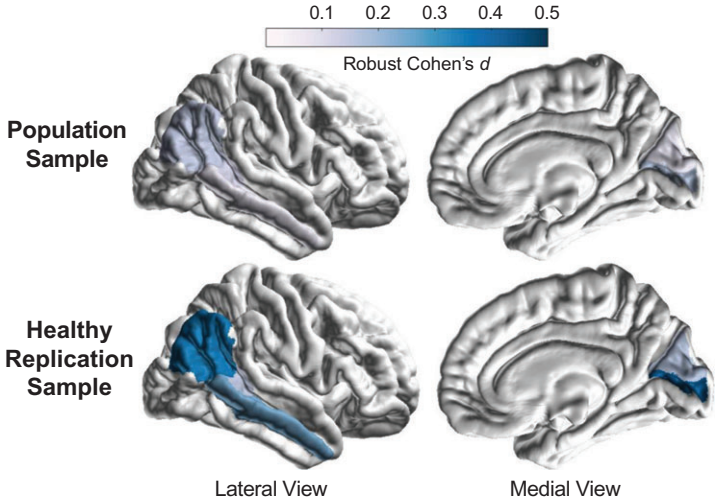

	Population Sample	Replication Sample
	Robust *d*	Robust *d*
IPL	0.15	0.35
PCAL	0.17	0.40
bSTS	0.12	0.15
MTG	0.07	0.25
CUN	0.08	0.17

Figure 4. Effect sizes of brain regions that differed by PSE using OLS regressions. Robust Cohen's *d*'s were acquired with the "akp.effect" function in R. Effect sizes shown here are independent of covariates in the model. Magnitude of effects can be interpreted according to Cohen's guidelines: 0.2 = small, 0.5 = medium, ≥0.5 = large (Wilcox, in press). IPL = inferior parietal, PCAL = pericalcarine, bSTS = banks of superior temporal sulcus, MTG = middle temporal gyrus, CUN = cuneus.

Table 2 Robust Effect Sizes of Brain Regions that Differed by PSE Using Quantile Regression

Region	a. Population sample		b. Healthy replication sample	
	QS effect	Difference score [CI]	QS effect	Difference score [CI]
Banks of Superior Temporal SA	0.53***	0.11 [0.06, 0.16]	0.55	0.15 [−0.11, 0.40]
Caudate VOL	0.53***	0.10 [0.05, 0.15]	0.55	0.22 [−0.10, 0.41]
Cuneus SA	0.52**	0.08 [0.03, 0.12]	0.55	0.18 [−0.06, 0.42]
Inferior Parietal SA	0.54***	0.15 [0.10, 0.20]	0.61**	0.36 [0.14, 0.59]
Inferior Temporal SA	0.52*	0.05 [0.00, 0.10]	0.54	0.16 [−0.06, 0.38]
Middle Temporal SA	0.52*	0.07 [0.15, 0.12]	0.57	0.25 [0.01, 0.49]
Pallidum VOL	0.52**	0.07 [0.02, 0.13]	0.55	0.14 [−0.10, 0.39]
Pericalcarine SA	0.55***	0.18 [0.13, 0.23]	0.61**	0.14 [0.14, 0.64]
Putamen VOL	0.49	−0.04 [−0.09, 0.01]	0.54	0.18 [−0.08, 0.43]
Rostral Middle Frontal SA	0.52*	0.06 [0.01, 0.12]	0.55	0.16 [−0.09, 0.41]

Note. Effect sizes were derived using Yuen's test for trimmed means ("yuenQS" function in R). A robust measure of "shift", or quantile shift effect (QS) was computed and can be interpreted as follows: Cohen's *d* = 0, 0.2, 0.5, and 0.8 corresponds to QS = 0.5, 0.55, 0.65, and 0.70, respectively (Wilcox, in press). Significant QS values indicate that we can reject the null hypothesis of equal distribution. QS values indicate the quantile to which the distribution has shifted from the population median (0.5). Cortical QS effects are plotted on a cortical map in Supplementary Figure 1. SA = surface area, VOL = volume. ***P < 0.001, **P < 0.01, *P < 0.05.

PSE$^+$ group. We did not replicate the effects of PSE in the bSTS or CUN, which were observed using the OLS approach (Fig. 3).

Quantile regressions also replicated the findings of lower SA in the PCAL and IPL in the PSE$^+$ group, specifically at quantiles 0.5–0.9 and 0.25–0.75, respectively (Fig. 2*b*, Supplementary Table 3). We did not replicate the effects of PSE in the bSTS, ITG, MTG, or RMFG, which were observed using the quantile regression method. We did not compute quantile regressions adjusting for birthweight in the elite healthy sample as the design matrix was computationally singular after adjusting for additional covariates.

Effect sizes were moderate in comparison to the discovery sample, particularly in the IPL (Robust d = 0.35) and PCAL (Robust d = 0.4) for OLS models (Fig. 4). This finding was also demonstrated with the quantile regressions (QS effects = 0.61), corresponding approximately to Cohen's *d*'s = 0.4 in the IPL and PCAL (Table 2*b*).

Disease Risk by PSE and Brain Structure

Logistic regressions revealed significant variability in disease risk for each predictor variable in our partial regression models. PSE was associated with increased risk of developing a CNS or psychiatric condition (RR = 29%), disease of the ear or mastoid process (RR = 63%), circulatory condition (RR = 12%), digestive condition (RR = 8%), or genitourinary condition (RR = 14%) (Supplementary Table 4). To determine whether the degree of neuroanatomical insult further contributed to disease risk, we examined the relative risk in the PSE$^+$ group after individually adding brain metrics that differed by PSE (SA in the PCAL, IPL, MTG, bSTS, ITG, RMFG, CUN) to the logistic models. Partial *F* tests revealed significantly better fit for each ICD-10 model with the addition of at least one SA metric to the predictor set (Supplementary Table 5). However, SA metrics themselves were not always significant predictors of the target condition

when also adjusting for all other predictors. For brevity, we describe the models in which regional SA metrics significantly improved model fit *and* significantly predicted the target condition at the 0.05 alpha level.

Analyses in the PSE^+ group revealed an 11% decreased risk for circulatory conditions ($p = 0.008$), and a 10% decreased risk for digestive ($p = 0.002$) and musculoskeletal conditions ($p = 0.038$) with each standard deviation increase in PCAL SA (Supplementary Table 6). We did not observe these relationships in the PSE^- group for circulatory or digestive conditions. Surprisingly, we did observe a 7% higher risk for musculoskeletal conditions with each standard deviation increase in PCAL SA in the PSE^- group ($p = 0.042$). The PSE^+ group also demonstrated an 11% decreased risk for circulatory and genitourinary conditions with each standard deviation increase in SA of the MTG and RMFG, respectively. Finally, the IPL, ITG, and MTG was associated with a 19%, 16%, and 15% decreased risk for endocrine conditions in the PSE^+ group with each standard deviation increase in SA. These risks were not observed in the PSE^- group. Across all logistic regressions where brain metrics improved model performance, the addition of the IPL as a predictor of endocrine conditions in the PSE^+ group showed the best model fit as determined by Akaike information criterion (AIC).

For interpretation, we examined the role of subclasses of the ICD-10 conditions identified above in relation to PSE. Greater SA in the PCAL and MTG was associated with lower risk for hypertensive disease in the PSE^+ (RR = 0.87 and 0.82, respectively) and PSE^- groups (RR = 0.90 and 0.83, respectively). Lower SA in the PCAL also was associated with a higher risk for non-infective gastroenteritis/colitis (RR = 0.72), colon polyps (RR = 0.63), and joint disorders (RR = 0.81) in the PSE^+ group only. Finally, lower SA in the RMFG was associated with higher risk for pelvic inflammatory disease (RR = 0.56), and endometrial polyps (RR = 0.50) among females in the PSE^+ group only (Supplementary Table 7). We did not observe a significant effect of SA on sub-classes of endocrine conditions in either PSE group.

Discussion

We report the first large-scale evidence of long-term cortical brain disruption among individuals perinatally exposed to tobacco smoke. Consistent with our hypothesis, SA measurements were more sensitive to PSE than CT or VOL. PSE^+ individuals demonstrated lower SA in occipito-parietal and temporal brain regions when compared to the PSE^- group, with the most robust effects observed in the pericalcarine (PCAL) and inferior parietal cortex (IPL). Cortical SA abnormalities in the PCAL, middle temporal gyrus (MTG), and rostral middle frontal gyrus (RMFG) were associated with significantly higher risk for disease among individuals in PSE^+ group, with the PCAL affecting risk for a broad set of disorders within the circulatory, digestive, and musculoskeletal systems. Importantly, lower SA in the PCAL and IPL was observed after adjusting for potential psychosocial and physiologic confounders in both the population-based sample and a hold-out replication sample of healthy adults, suggesting the observed relationships to PSE were not a downstream effect of intervening health conditions. Collectively, these findings highlight the long-term consequences of PSE on brain structure and disease risk later in life.

Cortical SA was most closely associated with PSE—consistent with the developmental timing of brain structure maturation in the perinatal period. Cortical maturation is sensitive to environmental exposures during this time, as the majority of cortical growth occurs between 21 weeks' gestational age and the first postnatal year (Gilmore et al. 2012). However, SA and CT follow distinct patterns of pre- and postnatal development and show consistently unique relationships with age. The majority of CT growth occurs during gestation, followed by an increase in CT around 40% and 0.7% during the first and second postnatal years, respectively. Changes in CT during the first postnatal year have been shown in nearly all regions except the central sulcus and calcarine fissure, with the lowest growth rates in visual, motor, and somatosensory cortices (Li et al. 2015). By contrast, the cortical surface expands by around 180% and 120% during the first and second postnatal year, with localized gains in temporal, parietal, and occipital cortices (Li et al. 2013). More recent work shows a 0.51% daily increase in SA and 0.09% daily increase in CT between 6 and 144 days after birth (Jha et al. 2018). Changes in cortical development after age 2 are primarily driven by cortical surface expansion (Lyall et al. 2015), suggesting there is an extended window of vulnerability of cortical SA to secondhand smoke and other environmental toxins beyond the perinatal period. This is consistent with several reports of monotonic decline of CT after age 3, though this pattern has not been universally identified across studies (for review see Walhovd et al. 2017). Data related to childhood and adolescent smoke exposure were not available for our study, but it is possible that our results reflect chronic effects of secondhand smoke that occurred throughout childhood development. Future studies will benefit from a more detailed assessment of early life environment that includes information on duration of exposure, frequency of smoking behaviors and number of smokers in the household.

The link between PSE and lower SA in the PCAL and IPL is consistent with animal studies that revealed altered brain development in the visual and somatosensory systems following prenatal nicotine exposure. The most prominent nAChR subunit in the human CNS is heteromeric α4β2, which binds nicotine with high affinity (Bansal et al. 2000). Earlier work using autoradiography in rats revealed a 90% and 107% increase in α4β2 density in the somatosensory and visual cortices, respectively, following prenatal nicotine administration (Tizabi and Perry 2000). Primate studies by Duncan et al. (2009; 2015) reported increased nAChR binding, including α4β2, in the medulla and primary visual cortex (V1) of fetal baboons. Receptor upregulation in these regions is believed to reflect the process of desensitization, increasing the risk for developmental perturbations (Ernst et al. 2001; Aoyama et al. 2016). Early postnatal smoke exposure also alters normal programming of the cholinergic system (Navarro et al. 1989; Yanai et al. 1992; Zahalka et al. 1992; Slotkin 2004; Heath and Picciotto 2009), which prior studies have linked to altered developmental plasticity, reduced cortical size, and attenuated maturation of cortical pyramidal neurons (Aramakis and Metherate 1998; Robertson et al. 1998). Developmental disruptions in cholinergic activity may explain lower cortical SA in the PCAL of exposed individuals in our study, as spectroscopy has revealed elevated choline in the PCAL of subjects with congenital blindness—a contrast to typically high choline levels at birth that decline with postnatal cortical maturation and pruning (Bluml et al. 2013). We suspect that abnormal developmental programming associated with PSE may be driven by epigenetic modifications that alter the biological response to stress and arrest normal brain maturation (Knopik et al. 2012). Epigenetic changes were not investigated here, but maternal tobacco use during pregnancy may disrupt epigenetic regulation by changes in DNA methylation (Toledo-Rodriguez et al. 2010; Ba et al. 2011; Suter

et al. 2011). Future studies examining longitudinal DNA methylation patterns among individuals exposed to PSE will clarify this possible connection.

Negative associations between SA in the PCAL and MTG and risk for circulatory conditions in the PSE$^+$ group extends prior work. In Tchistiakova et al. (2014), individuals with hypertension and type 2 diabetes demonstrated lower cerebrovascular reactivity in occipito-parietal cortices during successive breath holds, and lower thickness in the right occipital lobe. Autopsy analysis also has shown microinfarcts in the occipital cortex of brains with cerebral amyloid angiopathy—a cerebrovascular condition characterized by amyloid build-up in blood vessels of the CNS (Kovari et al. 2017). Prior work using structural MRI has revealed positive associations between CT in the MTG and cholesterol (Leritz et al. 2011), further supporting a role for vascular health on this brain region.

The link between SA in the PCAL and musculoskeletal conditions was not expected but may be partly explained by increased proteolysis through smoke-induced activation of inflammatory mediators. Exposure to cigarette smoke increases blood levels of proinflammatory cytokines such as tumor necrosis factor-α and interleukin-6 in animals, which can lead to muscle wasting by increased proteolysis and protein synthesis inhibition (Degens et al. 2015). Acetaldehyde, a Group 2B substance (*possibly carcinogenic*) and bioactive toxicant of mainstream and sidestream smoke, lowers the rate of protein synthesis in cultured human muscle cells (Hong-Brown et al. 2001). Excessive proteolysis via acetylaldehyde activation of matrix metalloproteins (MMPs) is sufficient to destroy articular cartilage in diseased joints (Rengel et al. 2007; Rose and Kooyman 2016), and may explain the increased risk for joint disorders in the PSE$^+$ group. Imbalanced proteolytic activity is also implicated in digestive conditions, as MMPs are the most abundant proteases in gut mucosa and are upregulated among individuals with ulcerative colitis (Pujada et al. 2017). While these mechanisms offer potential insights into links between PSE and disease, increased risk for these disorders as a function of the PCAL is not clear. Smoke-induced exposure to heavy metals (Otto and Fox 1993; Korogi et al. 1994; Braissant et al. 2013; Ekinci et al. 2014; Oeltzschner et al. 2015) is associated with biochemical disruptions to neurotransmitter systems, and it is possible that physiologic and neurostructural changes explain the link between the visual cortex and peripheral diseases of the digestive and musculoskeletal systems. Alternatively, the degree of SA disruption in the PCAL may be a marker of extant exposure, and there may not be a direct link between PSE and PCAL structure directly. Experimental studies are needed to determine the degree that toxins from secondhand smoke beyond nicotine influence central and peripheral biochemistry.

This study has several strengths. First, the large sample size boosted statistical power and allowed us to create a hold-out sample of healthy adults to test the reproducibility of our main findings. Replication analyses revealed a specific effect of PSE on the PCAL and IPL; stronger effect sizes in these regions in the healthy hold-out sample may indicate a more direct effect of PSE than other brain regions identified in the main analyses. Importantly, the replication sample was on average 3 years younger than the population-based sample, and may be at high risk for PCAL-associated diseases of the circulatory and digestive system with increasing age (PCAL-associated risk for musculoskeletal conditions did not show an aging effect). Although the IPL was not identified as a significant predictor of disease risk in this sample, SA in this region did improve model fit for diseases of the circulatory and respiratory systems. The lack of direct link may be due to low cell sizes for specific conditions within these larger ICD-10 categories.

Second, we used robust statistical methods to ensure the most accurate depiction of PSE brain effects. Part of this approach included the use of quantile regression models to examine the effect of PSE at various points along the distribution. By doing so, we observed additional region-specific effects of PSE in the inferior temporal gyrus (ITG) and rostral middle frontal gyrus (RMFG)—regions that were not captured using a standard regression approach. SA in these regions improved model fit for our logistic regression models of CNS and genitourinary conditions, respectively. The ITG did not show a significant individual relationship to CNS conditions, but higher SA in the RMFG was linked to a 44–50% lower risk of pelvic inflammatory disease (PID) and endometrial polyps in females of the PSE$^+$ group. This association may be partly explained by the increased risk for PID with increasing cardiovascular morbidities (Chen et al. 2011), the latter showing links to cerebral hypoperfusion in the RMFG (Hoscheidt et al. 2017). Of note, recent histological analysis of the human uterine cavity revealed positive associations between endometrial polyps and heavy metals such as lead, cadmium, aluminum, and nickel—trace elements found in tobacco smoke (Rzymski et al. 2016).

A significant limitation of this study is the self-reported and retrospective proxy measure of PSE. The participants' mothers were not asked about smoking behaviors during pregnancy given the older age range of participants (44-80 years) and likelihood that many mothers would be ill or deceased. Thus, knowledge of PSE was likely informed by a parent or other close relative. If informed by the mother, prior work shows high validity and reliability of self-reported smoking during pregnancy (George et al. 2006; Pickett et al. 2009) in both retrospective and prospective studies (Githens et al. 1993; Heath et al. 2003; Tomeo et al. 1999; Yawn et al. 1998). It has been shown that recall errors are almost always a result of under-reported maternal smoking behaviors (George et al. 2006; Pickett et al. 2009), attributable to poor emotional health (Pickett et al. 2009). As such, recall error that may have occurred in our study likely applied to participants who reported no PSE, not knowing about PSE, and those who did not answer the question. We expect that deliberate misrepresentation of PSE would be low to nonexistent in this sample given the removed introspective nature of the question and reduced desire to produce a socially acceptable response. Longitudinal birth cohort studies that assess parental self-report, as well as delayed retrospective recall of maternal smoking and related early life exposures, may be able to address recall accuracy in offspring to guide the design of future studies.

The prevalence of self-reported PSE in our study (~41%) is consistent with base rates of female smoking prevalence that occurred during the participants' birth years (1938-1974, average birth year = 1956). Epidemiological records show that nearly half of all women smoked by 1948, a number that remained relatively stable until the 1980's (Eliot 2001). Reports from the 1970 British Birth Cohort Study (BCS70) showed that approximately 46% of individuals born within a single week of 1970 (N > 16,000) were born to mothers who smoked at term (Rush and Cassano 1983)—a 12% increase from maternal smoking trends in the 1958 Birth Cohort Study. Additional work from BCS70 revealed that 45% of mothers resumed smoking immediately after giving birth (Chamberlain et al. 1978). This aligns with more recent work indicating that regular smoking mothers who quit smoking during pregnancy have a high likelihood of relapse within 6 months postpartum (Colman and Joyce 2003).

Finally, mothers who smoke at term and continue to smoke during the postnatal period are unlikely to quit smoking thereafter (Kahn et al. 2002). Thus, participants' recall may be influenced both by second-hand information provided by parents and relatives, and first-hand recall of smoking behaviors that continued through childhood and adolescence.

Maternal smoking behaviors also are complicated by generational factors such as parental educational attainment, paternal occupation, and SES (Hackman and Farah 2009; Hackman et al. 2010), but these measures were not recorded by UKB. Several studies show that mothers who smoke during pregnancy are less educated and of lower SES than non-smoking mothers (Fingerhut et al. 1990; Colman and Joyce 2003), which in turn is linked to negative health factors such as substance misuse, poor nutrition, sedentary activity, increased stress, poor mental health, and increased exposure to environmental toxins (Kramer et al. 2000). Each of these variables is independently associated with developmental brain and behavioral abnormalities that may have influenced the study findings (Hackman and Farah 2009). It is important to note, however, that relationships between cigarette smoking and SES in women did not emerge until the 1960's (Wald and Nicolaides-Bouman 1991)—several years after the average birth year of UKB participants. Still, we cannot exclude the possibility of concurrent substance use during pregnancy, particularly for licit substances such as alcohol. Alcohol contains many of the same toxins as cigarette smoke (e.g., aldehydes) and consumption during pregnancy imparts a similarly high risk to fetal brain development (Kitsiou-Tzeli and Tzetis 2017). Still, it is unlikely that light to moderate prenatal alcohol exposure was a primary driver of our results since the window of exposure is limited (9 months) when compared to the potential window of tobacco exposure that imposes high risk to brain development through adolescence and beyond. We attempted to account for these limitations by conducting a secondary analysis that covaried for birth weight, which prior studies have identified as a stable marker of prenatal health (Gortmaker 1979; Kogan et al. 1994; Alexander and Korenbrot 1995). These analyses revealed a nominal change in results, suggesting that our main findings were not confounded by other prenatal health factors. Further work is needed to determine the relative influence of postnatal factors on long-term cortical brain structure in relation to maternal smoking.

We also note that smoking initiation and regular smoking behaviors are heritable traits (for review see Do and Maes 2016), so participants whose mothers smoked may have inherited a greater aggregate risk from genetic variants that predispose to smoking initiation and persistence among smokers in this study compared to those whose mothers did not smoke. As such, the effect of PSE on imaging derived brain measures may partly result from smoking-associated genetic variants that were inherited among exposed participants. Finally, we cannot assess the causal directionality of disease risk for each brain measure in our logistic models given the descriptive nature of this design. Similarly, we do not know if our results will generalize to other populations, as this sample was specific to a UK population and disease prevalence in the UKB sample is lower, on average, than disease prevalence in other population-based cohorts (Fry et al. 2017).

Conclusion

This is the largest-ever neuroimaging study of the structural brain effects of PSE, and the first study examining smoke-related latent effects in a sample of middle and older-aged individuals. Our imaging and robust statistical approach revealed a dominant, system-specific effect of PSE on sensory brain structures later in life, with the most pronounced and clinically relevant abnormalities on cortical SA of the PCAL. The findings in this study are of high public health relevance given the current international tobacco crisis that is increasing in some low and middle income countries (WHO 2018). Given global increases in life expectancy, long-term effects of PSE may bring added morbidities and complicate quality of life in later adulthood. Further, the evolving landscape of cannabis legislation may pose many of the neuroanatomical consequences and overall health risks discussed here as a result of smoke exposure (Moir et al. 2008).

Supplementary Material

Supplementary material is available at *Cerebral Cortex* online.

Funding

This work was supported by the National Institutes of Health (grant numbers 1R01MH116147, 1R01AG059874, U54EB020403, 1R56AG058854, RF1AG041915, 2P41EB015922, RF1AG051710, P01AG026572, and NIMH R01MH117601).

Notes

This work was conducted using the UK Biobank Resource under Application Number 11 559. The UK Biobank was established by the Wellcome Trust, Medical Research Council, Department of Health and the Scottish Government. UK Biobank funding was also supported by the Welsh Assembly Government, British Heart Foundation, and Diabetes UK. Cortical processing and QC were supported by the ENIGMA pipeline (http://enigma.ini.usc.edu/protocols/imaging-protocols/). PT and NJ are MPI of a research related grant from Biogen, Inc for work unrelated to the contents of this manuscript. *Conflict of Interest*: None declared.

Appendix

Data Parser

Members of our group developed an algorithmic tool to facilitate ease of data extraction in UK Biobank (UKB); the tool can be found here https://github.com/USC-IGC/ukbb_parser. The parser was built in Python and is compatible with UKB datasets extracted under different application numbers; it also can be used as a template bio-parser for other large-scale databases. Predefined data filters have been developed for extraction of demographic (e.g., age, sex, ethnic background) and neuroimaging variables, and data fields related to self-reported and medically documented ICD-10 health conditions. The parser is continuously updated; updates are publicly available through GitHub (Zhu et al. 2019).

Statistical Strategy

All statistical analyses were completed in R version 3.4. The statistical functions described below are described in detail in the Wilcox Robust Statistical Functions (WRS2) package in R (Mair and Wilcox 2016).

Multivariate Outlier Detection

We built a robust statistical function in R to account for leverage points (outliers among the independent variables) and multivariate outliers (points among the dependent variable that are far from the true regression line) in our full statistical model. This involved several steps. First, we z-transformed each of our continuous independent variables (age, intracranial volume (ICV), waist-hip ratio (WHR), Townsend scores, and the first 4 multidimensional scaling components of genetic ancestry (C1-C4) as is common in genetic studies such as Hibar et al. (2015) to create a standardized scale for interpreting beta weights. Then, we created 2 matrices of independent variables: 1) matrix of all independent variables (categorical and continuous), and a 2) matrix of the continuous z-transformed independent variables using the function. To detect outliers among the continuous predictor set, we used the outpro function in the WRS2 package; the code is detailed here https://rdrr.io/rforge/WRS2/src/R/outpro.R.

The outpro function uses a modification of the Stahel-Donoho projection method—a robust estimator of multivariate location (Stahel 1981)—to detect multivariate outliers and leverage points. The basic idea is to determine the center of a given data cloud and project each data point to its center; outliers are detected based on relative distances between projection points. Once outliers and leverage points were removed from the continuous data matrix, we merged the remaining data with discrete predictors from the complete matrix of independent variables. These steps can be followed sequentially using the following code:

```
AD = cbind()                  #bind all predictors
CIV = cbind()                 #bind only the continuous predictors
id = outpro(CIV)$keep         #remove outliers and leverage points from
                                continuous data matrix
FD = AD[id,]                  #merge remaining data with discrete
                                predictors
(FD,y[id,])                   #merge outlier free predictor matrix with
                                Y outcome for analysis
```

Finally, we used (FD,y[id]) to retain the y values corresponding to the remaining data; this code was used in all statistical models that examined full model effects on the regions of interest.

Measuring Central Tendency

We examined the distribution of the imaging variables in the whole sample and between the exposed and unexposed maternal smoking groups using Kolmogorov–Smirnov (Massey 1952) and Koenker–Bassett tests (Koenker and Bassett 1982). The Kolmogorov–Smirnov test is a robust function for testing the maximum absolute differences in the distributions of 2 independent groups, and therefore does not require assumptions of central tendency. It is an ideal statistic for large samples as it is sensitive to differences at any point along the distribution. We used the Koenker–Bassett method to test the hypothesis of homoscedasticity between slopes at the 0.2 and 0.8 quantiles along the regression line and tested with 100 bootstrap samples by default. The R functions, inclusive of our outlier-free data matrix are below:

```
ks<-function(FD,y[id]),w=FALSE,sig=TRUE,alpha=.05))
qhomtv2<-function(x,y,nboot=100,alpha=.05,qval=c(.2,.8))
```

Collectively our results from these tests showed significant differences in the imaging distributions between the exposed and unexposed groups after adjusting for covariates.

Main Analyses

The neuroscience literature predominantly uses ordinary least squares (OLS) regressions for hypothesis testing. Therefore, we ran OLS regressions with an HC4 standard error estimator to enable direct comparisons to the existing literature using the function:

```
olshc4(FD,y[id])
```

As noted in the main text, the HC4 method performs relatively well under heteroscedasticity, but is highly conservative with a null rejection rate at ~1% (Cribari-Neto et al., 2014). Moreover, OLS can be negatively impacted by outliers. Thus, we used quantile regressions to test whether group differences existed at specific points along the distribution. The regci function (below) allowed us to test the hypothesis that predictor slopes were not equal to zero using the (conditional) quantiles = 0.1, 0.25, 0.5, 0.75, 0.9 associated with the dependent variable.

```
regci(FD,y[id],regfun=qreg,q=qval)
```

Estimates of Effect Size

Standard computations of effect size are inappropriate for data that are not normal and heteroscedastic. This is further complicated in models in models containing discrete and continuous predictors. Because our model included several discrete predictors (PSE, sex, college education, smoking status), we chose multiple methods to inform multivariate estimates of effect size. For both OLS and quantile regression models, we computed standardized beta weights for each individual predictor (Figures 1–3), which reflect the individual effect size of each predictor as a function of the multivariate model.

OLS Regression Models

We used least angle regression LASSO (least absolute shrinkage and selection operator) to sort predictors in order of importance, which uses beta weights, standard errors, and confidence intervals to determine the rank of each variable. This can be done in R using the larsR function, described by Efron et al. (2004). We chose this method over other LASSO methods because it automatically computes R^2—a multivariate index of model fit that would be most interpretable to readers. Variable rankings of significant OLS models are depicted in Figures 1 and 3. These figures depict the effect sizes of each predictor variable according to beta weights and relative feature rank; model effect sizes are indicated by R^2.

For group comparisons, we computed robust analogs of Cohen's *d* (Algina et al. 2005) to determine robust effect size estimates of the PSE variable on the individual ROIs (Fig. 4). To do this we used the akp.effect function in R, which is based on 20% trimmed means and Winsorized standard deviations. Many studies show that when comparing means, outliers and skewed distributions are a serious concern (Wilcox 1992, 1995; Crawford et al. 2006; Buzsaki and Mizuseki 2014; Nord et al. 2017; Szucs and Ioannidis 2017). Under normality, the standard error of a 20% trimmed mean is only slightly larger than the standard error of the full distribution's mean, but a slight shift from a normal distribution towards a heavy-tailed distribution can result in the mean having a much larger standard error. This effect can be seen even in the absence of outliers. Thus,

when testing hypotheses, little power is lost under normality, but substantially higher power might be achieved using a 20% trimmed mean because more accurate confidence intervals can be computed (Wilcox and Serang 2017). Concerns about normality decrease as the amount of trimming increases (Wilcox and Keselman, 2003; Wilcox and Rousselet 2018). Simulation studies show that a 20% trimmed mean is the recommended trimming for the appropriate balance between type 1 error and power across many nonnormal distributions, and in small samples ($n < 20$; Wilcox 1995b). Of note, the median is a trimmed mean based on the maximum amount of trimming (50%); prior work shows that the median can have a smaller standard error than the mean in distributions with thicker tails than the normal distribution (Rousselet et al. 2017; Wilcox and Serang 2017).

Although smaller trimmed means (e.g., 10%) can be used, the 20% trimmed mean is more reliable (Wilcox 1995a). Currently there is no known diagnostic that would provide compelling evidence that a smaller trimmed mean would be preferable, except perhaps in very sample sizes ($n < 5$; Ozdemir et al. 2013). Transforming the data (e.g., taking logs) is known to be relatively ineffective method for dealing with skewed distributions (Wilcox and Rousselet 2018).

Quantile Regression Models

Quantile regressions are more complicated than OLS, with different assumptions and limitations for determining univariate and multivariate estimates of effect size. In this study we used beta weights to determine the relative importance of each individual predictor at each conditional quantile (Fig. 2). We computed univariate estimates of *quantile shift* (QS) using yuenQS in R (Wilcox, in press). As described in the manuscript, a QS effect size reflects a shift of location based on the median of the typical difference of the distribution between 2 groups and deals with non-normality and heteroscedasticity. It represents how far the median of the typical difference (D) differs from the situation where the median is zero. If groups have identical distributions, $D = X\text{-}Y$ is symmetric about zero, the 0.5 quantile. A QS shift, say to QS = 0.6, indicates that the median of D corresponds to a shift to the 0.6 quantile when the groups have identical distributions. Thus, it captures the spirit of Cohen's d without specifying any family of distributions. In particular, it does not require or assume normality. Quantile shift effect sizes are depicted in Table 2. Currently there is no clear method for evaluating multivariate effect size for quantile regressions fit with robust methods.

References

Alexander GR, Korenbrot CC. 1995. The role of prenatal care in preventing low birth weight. Future Child. 5:103–120.

Alfaro-Almagro F, Jenkinson M, Bangerter NK, Andersson JLR, Griffanti L, Douaud G, Sotiropoulos SN, Jbabdi S, Hernandez-Fernandez M, Vallee E, et al. 2018. Image processing and quality control for the first 10,000 brain imaging datasets from UK Biobank. Neuroimage. 166:400–424.

Algina J, Keselman HJ, Penfield RD. 2005. An alternative to Cohen's standardized mean difference effect size: a robust parameter and confidence interval in the two independent groups case. Psychol Methods. 10:317–328.

Aoyama Y, Toriumi K, Mouri A, Hattori T, Ueda E, Shimato A, Sakakibara N, Soh Y, Mamiya T, Nagai T, et al. 2016. Prenatal nicotine exposure impairs the proliferation of neuronal progenitors, leading to fewer glutamatergic neurons in the medial prefrontal cortex. Neuropsychopharmacol. 41(2):578.

Aramakis VB, Metherate R. 1998. Nicotine selectively enhances NMDA receptor-mediated synaptic transmission during postnatal development in sensory neocortex. J Neurosci. 18: 8485–8495.

Aztiria E, Gotti C, Domenici L. 2004. Alpha7 but not alpha4 AChR subunit expression is regulated by light in developing primary visual cortex. J Comp Neurol. 480:378–391.

Ba Y, Yu H, Liu F, Geng X, Zhu C, Zhu Q, Zheng T, Ma S, Wang G, Li Z, et al. 2011. Relationship of folate, vitamin B12 and methylation of insulin-like growth factor-II in maternal and cord blood. Eur J Clin Nutr. 65:480–485.

Bansal A, Singer JH, Hwang BJ, Xu W, Beaudet A, Feller MB. 2000. Mice lacking specific nicotinic acetylcholine receptor subunits exhibit dramatically altered spontaneous activity patterns and reveal a limited role for retinal waves in forming ON and OFF circuits in the inner retina. J Neurosci. 20: 7672–7681.

Benjamini Y, Hochberg Y. 1995. Controlling the false discovery rate: a practical and powerful approach to multiple testing. J Roy Stat Soc B Met. 1:289–300.

Berridge MS, Apana SM, Nagano KK, Berridge CE, Leisure GP, Boswell MV. 2010. Smoking produces rapid rise of [11C]nicotine in human brain. Psychopharmacology (Berl). 209:383–394.

Blood-Siegfried J, Rende EK. 2010. The long-term effects of prenatal nicotine exposure on neurologic development. J Midwifery Womens Health. 55:143–152.

Bluml S, Wisnowski JL, Nelson MD Jr., Paquette L, Gilles FH, Kinney HC, Panigrahy A. 2013. Metabolic maturation of the human brain from birth through adolescence: Insights from in vivo magnetic resonance spectroscopy. Cereb Cortex. 23: 2944–2955.

Bouthoorn SH, van Lenthe FJ, Hokken-Koelega AC, Moll HA, Tiemeier H, Hofman A, Mackenbach JP, Jaddoe VW, Raat H. 2012. Head circumference of infants born to mothers with different educational levels; the Generation R Study. PLoS One. 7(6):e39798.

Braissant O, McLin VA, Cudalbu C. 2013. Ammonia toxicity to the brain. J Inherit Metab Dis. 36:595–612.

Buzsaki G, Mizuseki K. 2014. The log-dynamic brain: how skewed distributions affect network operations. Nat Rev Neurosci. 15:264–278.

Chamberlain G, Phillipp E, Howlett B, Masters K. 1978. British Births 1970. London: Heinemann.

Chatterton Z, Hartley BJ, Seok MH, Mendelev N, Chen S, Milekic M, Rosoklija G, Stankov A, Trencevsja-Ivanovska I, Brennand K, et al. 2017. In utero exposure to maternal smoking is associated with DNA methylation alterations and reduced neuronal content in the developing fetal brain. Epigenetics Chromatin. 10:4.

Chen PC, Tseng TC, Hsieh JY, Lin HW. 2011. Association between stroke and patients with pelvic inflammatory disease: a nationwide population-based study in Taiwan. Stroke. 42:2074–2076.

Choi S, Krishnan J, Ruckmani K. 2017. Cigarette smoke and related risk factors in neurological disorders: An update. Biomed Pharmacother. 85:79–86.

Coggins CR, McKinney WJ Jr, Oldham MJ. 2013. A comprehensive evaluation of the toxicology of experimental, nonfiltered cigarettes manufactured with different circumferences. Inhal Toxicol. 25(sup2):69–72.

Colman GJ, Joyce T. 2003. Trends in smoking before, during, and after pregnancy in ten states. Am J Prev Med. 24(1):29–35.

Crawford JR, Garthwaite PH, Azzalini A, Howell DC, Laws KR. 2006. Testing for a deficit in single-case studies: effects of departures from normality. Neuropsychologia. 44(4):666–677.

Cribari-Neto F. 2004. Asymptotic inference under heteroskedasticity of unknown form. Comput Stat Data An. 45:215–233.

Cribari-Neto F, Maria, da Gloria AL. 2014. New heteroskedasticity-robust standard errors for the linear regression model. Braz J Probab Stat. 28:83–95.

Degens H, Gayan-Ramirez G, van Hees HW. 2015. Smoking-induced skeletal muscle dysfunction: from evidence to mechanisms. Am J Respir Crit Care Med. 191:620–625.

Derauf C, Lester BM, Neyzi N, Kekatpure M, Gracia L, Davis J, Kallianpur K, Efird JT, Kosofsky B. 2012. Subcortical and cortical structural central nervous system changes and attention processing deficits in preschool-aged children with prenatal methamphetamine and tobacco exposure. Dev Neurosci. 34:327–341. choi.

Desikan RS, Segonne F, Fischl B, Quinn BT, Dickerson BC, Blacker D, Buckner RL, Dale AM, Maguire RP, Hyman BT, et al. 2006. An automated labeling system for subdividing the human cerebral cortex on MRI scans into gyral based regions of interest. Neuroimage. 31:968–980.

Ding G, Yu J, Chen Y, Vinturache A, Pang Y, Zhang J. 2017. Maternal smoking during pregnancy and necrotizing enterocolitis-associated infant mortality in preterm babies. Sci Rep UK. 7:45784.

Diver WR, Jacobs EJ, Gapstur SM. 2018. Secondhand smoke exposure in childhood and adulthood in relation to adult mortality among never smokers. Am J Prev Med. 55:345–352.

Do EK, Maes HH. 2016. Genotype × environment interaction in smoking behaviors: A systematic review. Nicotine Tob Res. 19(4):387–400.

Duncan JR, Garland M, Myers MM, Fifer WP, Yang M, Kinney HC, Stark RI. 2009. Prenatal nicotine-exposure alters fetal autonomic activity and medullary neurotransmitter receptors: Implications for sudden infant death syndrome. J Appl Physiol. 107(5):1579–1590.

Duncan JR, Garland M, Stark RI, Myers MM, Fifer WP, Mokler DJ, Kinney HC. 2015. Prenatal nicotine exposure selectively affects nicotinic receptor expression in primary and associative visual cortices of the fetal baboon. Brain Pathol. 25: 171–181.

Efron E, Hastie T, Johnstone I, Tibshirani R. 2004. Least angle regression. Ann Stat. 32:407–499.

Ekinci M, Ceylan E, Cagatay HH, Keles S, Altinkaynak H, Kartal B, Koban Y, Huseyinoglu N. 2014. Occupational exposure to lead decreases macular, choroidal, and retinal nerve fiber layer thickness in industrial battery workers. Curr Eye Res. 39:853–858.

El Marroun H, Schmidt MN, Franken IH, Jaddoe VW, Hofman A, van der Lugt A, Verhulst FC, Tiemeier H, White T. 2014. Prenatal tobacco exposure and brain morphology: A prospective study in young children. Neuropsychopharmacol. 39:792–800.

Eliot RE 2001. Destructive but sweet: Cigarette smoking among women 1890-1990 [dissertation]. [Glasgow (Scotland)]: University of Glasgow.

Ernst M, Moolchan ET, Robinson ML. 2001. Behavioral and neural consequences of prenatal exposure to nicotine. J Am Acad Child Adolesc Psychiatry. 40:630–641.

Fingerhut LA, Kleinman JC, Kendrick JS. 1990. Smoking before, during, and after pregnancy. Am J Public Health. 80(5): 541–544.

Fischl B. 2012. FreeSurfer. Neuroimage. 62:774–781.

Fry A, Littlejohns TJ, Sudlow C, Doherty N, Adamska L, Sprosen T, Collins R, Allen NE. 2017. Comparison of sociodemographic and health-related characteristics of UK Biobank participants with those of the general population. Am J Epidemiol. 186(9):1026–1034.

Gadekar T, Dudeja P, Basu I, Vashisht S, Mukherji S. 2018. Correlation of visceral body fat with waist-hip ratio, waist circumference and body mass index in healthy adults: a cross sectional study. Med J Armed Forces India.

George L, Granath F, Johansson AL, Cnattingius S. 2006. Self-reported nicotine exposure and plasma levels of cotinine in early and late pregnancy. Acta Obstet Gyn Scan. 85(11): 1331–1337.

Gilmore JH, Shi F, Woolson SL, Knickmeyer RC, Short SJ, Lin W, Zhu H, Hamer RM, Styner M, Shen D. 2012. Longitudinal development of cortical and subcortical gray matter from birth to 2 years. Cereb Cortex. 22:2478–2485.

Githens PB, Glass CA, Sloan FA, Entman SS. 1993. Maternal recall and medical records: an examination of events during pregnancy, childbirth, and early infancy. Birth. 20(3): 136–141.

Gortmaker SL. 1979. The effects of prenatal care upon the health of the newborn. Am J Public Health. 69:653–660.

Gotti C, Zoli M, Clementi F. 2006. Brain nicotinic acetylcholine receptors: native subtypes and their relevance. Trends Pharmacol Sci. 27:482–491.

Goujon A, Samir KC, Speringer M, Barakat B, Potancoková M, Eder J, Striessnig E, Bauer R, Lutz W. 2016. A harmonized dataset on global educational attainment between 1970 and 2060–An analytical window into recent trends and future prospects in human capital development. J Demogr Econ. 82 (3):315–363.

Hackman DA, Farah MJ. 2009. Socioeconomic status and the developing brain. Trends Cogn Sci. 13(2):65–73.

Hackman DA, Farah MJ, Meaney MJ. 2010. Socioeconomic status and the brain: Mechanistic insights from human and animal research. Nat Rev Neurosci. 11(9):651.

Heath AC, Knopik VS, Madden PA, Neuman RJ, Lynskey MJ, Slutske WS, Jacob T, Martin NG. 2003. Accuracy of mothers' retrospective reports of smoking during pregnancy: Comparison with twin sister informant ratings. Twin Res Hum Genet. 6(4):297–301.

Heath CJ, Picciotto MR. 2009. Nicotine-induced plasticity during development: Modulation of the cholinergic system and long-term consequences for circuits involved in attention and sensory processing. Neuropharmacol. 56:254–262.

Hibar DP, Stein JL, Renteria ME, Arias-Vasquez A, Desrivières S, Jahanshad N, Toro R, Wittfeld K, Abramovic L, Aribisala BS, et al. 2015. Common genetic variants influence human subcortical brain structures. Nature. 520(7546):224.

Hill WD, Hagenaars SP, Marioni RE, Harris SE, Liewald DC, Davies G, Okbay A, McIntosh AM, Gale CR, Deary IJ. 2016. Molecular genetic contributions to social deprivation and household income in UK Biobank. Curr Biol. 26(22):3083–3089.

Hofhuis W, de Jongste JC, Merkus PJ. 2003. Adverse health effects of prenatal and postnatal tobacco smoke exposure on children. Arch Dis Child. 88:1086–1090.

Holford TR, Meza R, Warner KE, Meernik C, Jeon J, Moolgavkar SH, Levy DT. 2014. Tobacco control and the reduction in smoking-related premature deaths in the United States, 1964-2012. JAMA. 311(2):164–171.

Hong-Brown LQ, Frost RA, Lang CH. 2001. Alcohol impairs protein synthesis and degradation in cultured skeletal muscle cells. Alcohol Clin Exp Res. 25:1373–1382.

Hoscheidt SM, Kellawan JM, Berman SE, Rivera-Rivera LA, Krause RA, Oh JM, Beeri MS, Rowley HA, Wieben O, Carlsson CM, et al. 2017. Insulin resistance is associated with lower arterial blood flow and reduced cortical perfusion in cognitively asymptomatic middle-aged adults. J Cereb Blood Flow Metab. 37:2249–2261.

Jha SC, Xia K, Ahn M, Girault JB, Li G, Wang L, Shen D, Zou F, Zhu H, Styner M, et al. 2018. Environmental influences on infant cortical thickness and surface area. Cereb Cortex. DOI:10.1093/cercor/bhy1020.

Kahn RS, Certain L, Whitaker RC. 2002. A reexamination of smoking before, during, and after pregnancy. Am J Public Health. 92(11):1801–1808.

Kitsiou-Tzeli S, Tzetis M. 2017. Maternal epigenetics and fetal and neonatal growth. Curr Opin Endocrinol. 24(1):43–46.

Knopik VS, Maccani MA, Francazio S, McGeary JE. 2012. The epigenetics of maternal cigarette smoking during pregnancy and effects on child development. Dev Psychopathol. 24: 1377–1390.

Koenker R, Bassett G Jr. 1982. Robust tests for heteroscedasticity based on regression quantiles. Econometrica. 1:43–61.

Kogan MD, Alexander GR, Kotelchuck M, Nagey DA. 1994. Relation of the content of prenatal care to the risk of low birth weight: Maternal reports of health behavior advice and initial prenatal care procedures. JAMA. 271(17):1340–1345.

Korogi Y, Takahashi M, Shinzato J, Okajima T. 1994. MR findings in seven patients with organic mercury poisoning (Minamata disease). Am J Neuroradiol. 15:1575–1578.

Kovari E, Herrmann FR, Gold G, Hof PR, Charidimou A. 2017. Association of cortical microinfarcts and cerebral small vessel pathology in the ageing brain. Neuropathol Appl Neurobiol. 43:505–513.

Kramer MS, Seguin L, Lydon J, Goulet L. 2000. Socio-economic disparities in pregnancy outcome: why do the poor fare so poorly? Paediatr Perinat Ep. 14(3):194–210.

Lee HJ, Hwang SY, Hong HC, Ryu JY, Seo JA, Kim SG, Kim NH, Choi DS, Baik SH, Choi KM, et al. 2015. Waist-to-hip ratio is better at predicting subclinical atherosclerosis than body mass index and waist circumference in postmenopausal women. Maturitas. 80:323–328.

Leritz EC, Salat DH, Williams VJ, Schnyer DM, Rudolph JL, Lipsitz L, Fischl B, McGlinchey RE, Milberg WP. 2011. Thickness of the human cerebral cortex is associated with metrics of cerebrovascular health in a normative sample of community dwelling older adults. Neuroimage. 54:2659–2671.

Li G, Lin W, Gilmore JH, Shen D. 2015. Spatial patterns, longitudinal development, and hemispheric asymmetries of cortical thickness in infants from birth to 2 years of age. J Neurosci. 35(24):9150–9162.

Li G, Nie J, Wang L, Shi F, Lin W, Gilmore JH, Shen D. 2013. Mapping region-specific longitudinal cortical surface expansion from birth to 2 years of age. Cereb Cortex. 23: 2724–2733.

Liu J, Lester BM, Neyzi N, Sheinkopf SJ, Gracia L, Kekatpure M, Kosofsky BE. 2013. Regional brain morphometry and impulsivity in adolescents following prenatal exposure to cocaine and tobacco. JAMA Pediatr. 167:348–354.

Lyall AE, Shi F, Geng X, Woolson S, Li G, Wang L, Hamer RM, Shen D, Gilmore JH. 2015. Dynamic development of regional cortical thickness and surface area in early childhood. Cereb Cortex. 25(8):2204–2212.

Mair P, Wilcox R 2016. Robust statistical methods in r using the wrs2 package. Harvard Univ., Cambridge, MA, USA, *Tech. Rep*.

Massey FJ. 1952. Distribution table for the deviation between two sample cumulatives. Ann Math Statist. 23:435–441.

Medina-Inojosa JR, Batsis JA, Supervia M, Somers VK, Thomas RJ, Jenkins S, Grimes C, Lopez-Jimenez F. 2018. Relation of waist-hip ratio to long-term cardiovascular events in patients with coronary artery disease. Am J Cardiol. 121: 903–909.

Metherate R, Hsieh CY. 2003. Regulation of glutamate synapses by nicotinic acetylcholine receptors in auditory cortex. Neurobiol Learn Mem. 80:285–290.

Miller KL, Alfaro-Almagro F, Bangerter NK, Thomas DL, Yacoub E, Xu J, Bartsch AJ, Jbabdi S, Sotiropoulos SN, Andersson JL, et al. 2016. Multimodal population brain imaging in the UK Biobank prospective epidemiological study. Nat Neurosci. 19:1523–1536.

Moir D, Rickert WS, Levasseur G, Larose Y, Maertens R, White P, Desjardins S. 2008. A comparison of mainstream and sidestream marijuana and tobacco cigarette smoke produced under two machine smoking conditions. Chem Res Toxicol. 21(2):494–502.

Mousavi SV, Mohebi R, Mozaffary A, Sheikholeslami F, Azizi F, Hadaegh F. 2015. Changes in body mass index, waist and hip circumferences, waist to hip ratio and risk of all-cause mortality in men. Eur J Clin Nutr. 69:927–932.

Navarro HA, Seidler FJ, Eylers JP, Baker FE, Dobbins SS, Lappi SE, Slotkin TA. 1989. Effects of prenatal nicotine exposure on development of central and peripheral cholinergic neurotransmitter systems. Evidence for cholinergic trophic influences in developing brain. J Pharmacol Exp Ther. 251:894–900.

Nord CL, Valton V, Wood J, Roiser JP. 2017. Power-up: a reanalysis of 'power failure' in neuroscience using mixture modelling. J Neurosci. 3592–16.

Oeltzschner G, Butz M, Baumgarten TJ, Hoogenboom N, Wittsack HJ, Schnitzler A. 2015. Low visual cortex GABA levels in hepatic encephalopathy: links to blood ammonia, critical flicker frequency, and brain osmolytes. Metab Brain Dis. 30:1429–1438.

Orr-Urtreger A, Broide RS, Kasten MR, Dang H, Dani JA, Beaudet AL, Patrick JW. 2000. Mice homozygous for the L250T mutation in the alpha7 nicotinic acetylcholine receptor show increased neuronal apoptosis and die within 1 day of birth. J Neurochem. 74:2154–2166.

Otto DA, Fox DA. 1993. Auditory and visual dysfunction following lead exposure. Neurotoxicol. 14:191–207.

Ozdemir AF, Wilcox RR, Yildiztepe E. 2013. Comparing measures of location: Some small-sample results when distributions differ in skewness and kurtosis under heterogeneity of variances. Commun Stat-Simul C. 42(2):407–424.

O'Leary KT, Loughlin SE, Chen Y, Leslie FM. 2008. Nicotinic acetylcholine receptor subunit mRNA expression in adult and developing rat medullary catecholamine neurons. J Comp Neurol. 510:655–672.

Patenaude B, Smith SM, Kennedy DN, Jenkinson M. 2011. A Bayesian model of shape and appearance for subcortical brain segmentation. Neuroimage. 56:907–922.

Pickett KE, Kasza K, Biesecker G, Wright RJ, Wakschlag LS. 2009. Women who remember, women who do not: a methodological study of maternal recall of smoking in pregnancy. Nicotine Tob Res. 11(10):1166–1174.

Polanska K, Hanke W, Ronchetti R, Hazel P, Zuurbier M, Koppe JG, Bartonova A. 2008. Environmental tobacco smoke exposure and children's health. Acta Paediatrica. 95:86–92.

Pujada A, Walter L, Patel A, Bui TA, Zhang Z, Zhang Y, Denning TL, Garg P. 2017. Matrix metalloproteinase MMP9 maintains

epithelial barrier function and preserves mucosal lining in colitis associated cancer. Oncotarget. 8:94650–94665.

Rengel Y, Ospelt C, Gay S. 2007. Proteinases in the joint: clinical relevance of proteinases in joint destruction. Arthritis Res Ther. 9:221.

Robertson RT, Gallardo KA, Claytor KJ, Ha DH, Ku KH, Yu BP, Lauterborn JC, Wiley RG, Yu J, Gall CM, et al. 1998. Neonatal treatment with 192 IgG-saporin produces long-term forebrain cholinergic deficits and reduces dendritic branching and spine density of neocortical pyramidal neurons. Cereb Cortex. 8(2):142–155.

Rose BJ, Kooyman DL. 2016. A tale of two joints: the role of matrix metalloproteases in cartilage biology. Dis Markers.

Rousselet GA, Pernet CR, Wilcox RR. 2017. Beyond differences in means: robust graphical methods to compare two groups in neuroscience. *Eur*. J Neuroscience. 46(2):1738–1748.

Rush D, Cassano P. 1983. Relationship of cigarette smoking and social class to birth weight and perinatal mortality among all births in Britain, 5-11 April 1970. J Epidemiol Commun H. 37(4):249–255.

Rzymski P, Niedzielski P, Rzymski P, Tomczyk K, Kozak L, Poniedzialek B. 2016. Metal accumulation in the human uterus varies by pathology and smoking status. Fertil Steril. 105(6):1511–1518.

Santos S, Severo M, Gaillard R, Santos AC, Barros H, Oliveira A. 2016. The role of prenatal exposures on body fat patterns at 7 years: intrauterine programming or birthweight effects? Nutr Metab Cardiovasc Dis. 26:1004–1010.

Scicali R, Rosenbaum D, Di Pino A, Giral P, Cluzel P, Redheuil A, Piro S, Rabuazzo AM, Purrello F, Bruckert E, et al. 2018. An increased waist-to-hip ratio is a key determinant of atherosclerotic burden in overweight subjects. Acta Diabetol. 55:741–749.

Singh N, Gupta VK, Kumar A, Sharma B. 2017. Synergistic effects of heavy metals and pesticides in living systems. Front Chem. 5:70.

Slotkin TA. 2004. Cholinergic systems in brain development and disruption by neurotoxicants: nicotine, environmental tobacco smoke, organophosphates. Toxicol Appl Pharmacol. 198:132–151.

Smith GD, Whitley E, Dorling D, Gunnell D. 2001. Area based measures of social and economic circumstances: cause specific mortality patterns depend on the choice of index. J Epidemiol Community Health. 55:149–150.

Stahel WA 1981. Breakdown of covariances estimators. Research Report 31 Fachgruppe für Statistik, E.T.H. Zürich.

Streng KW, Voors AA, Hillege HL, Anker SD, Cleland JG, Dickstein K, Filippatos G, Metra M, Ng LL, Ponikowski P, et al. 2018. Waist-to-hip ratio and mortality in heart failure. Eur J Heart Fail. 20:1269–1277.

Suter M, Ma J, Harris A, Patterson L, Brown KA, Shope C, Showalter L, Abramovici A, Aagaard-Tillery KM. 2011. Maternal tobacco use modestly alters correlated epigenome-wide placental DNA methylation and gene expression. Epigenetics. 6:1284–1294.

Swan GE, Lessov-Schlaggar CN. 2007. The effects of tobacco smoke and nicotine on cognition and the brain. Neuropsychol Rev. 17(3):259–273.

Szucs D, Ioannidis J. 2017. When null hypothesis significance testing is unsuitable for research: A reassessment. Front Hum Neurosci. 11:390.

Tchistiakova E, Anderson ND, Greenwood CE, MacIntosh BJ. 2014. Combined effects of type 2 diabetes and hypertension associated with cortical thinning and impaired cerebrovascular reactivity relative to hypertension alone in older adults. Neuroimage Clin. 5:36–41.

Tizabi Y, Perry DC. 2000. Prenatal nicotine exposure is associated with an increase in [125I]epibatidine binding in discrete cortical regions in rats. Pharmacol Biochem Behav. 67: 319–323.

Toledo-Rodriguez M, Lotfipour S, Leonard G, Perron M, Richer L, Veillette S, Pausova Z, Paus T. 2010. Maternal smoking during pregnancy is associated with epigenetic modifications of the brain-derived neurotrophic factor-6 exon in adolescent offspring. Am J Med Genet B Neuropsychiatr Genet. 153B: 1350–1354.

Tomeo CA, Rich-Edwards JW, Michels KB, Berkey CS, Hunter DJ, Frazier AL, Willett WC, Buka SL. 1999. Reproducibility and validity of maternal recall of pregnancy-related events. Epidemiology. 1:774–777.

Toro R, Leonard G, Lerner JV, Lerner RM, Perron M, Pike GB, Richer L, Veillette S, Pausova Z, Paus T. 2008. Prenatal exposure to maternal cigarette smoking and the adolescent cerebral cortex. Neuropsychopharmacol. 33:1019–1027.

Townsend P, Phillimore P, Beattie A. 1988. Health and Deprivation: Inequality and the North. Routledge.

Wald NJ, Nicolaides-Bouman A. 1991. UK Smoking Statistics. 2nd ed. Oxford: Oxford University Press.

Walhovd KB, Fjell AM, Giedd J, Dale AM, Brown TT. 2017. Through thick and thin: a need to reconcile contradictory results on trajectories in human cortical development. Cereb Cortex. 27(2):1472–1481.

Wilcox RR. 1992. Why can methods for comparing means have relatively low power, and what can you do to correct the problem? Curr Dir Psychol Sci. 1(3):101–105.

Wilcox R. 1995a. Three multiple comparison procedures for trimmed means. Biometrical J. 37(6):643–656.

Wilcox RR. 1995b. Simulation results on solutions to the multivariate Behrens-Fisher problem via trimmed means. Statistician. 213–225.

Wilcox RR. 1995c. ANOVA: The practical importance of heteroscedastic methods, using trimmed means versus means, and designing simulation studies. Br J Math Stat Psychol. 48: 99–114.

Wilcox RR. 1996. Statistics for the social sciences. Academic Press.

Wilcox RR. in press. A robust nonparametric measure of effect size based on an analog of Cohen's d, plus inferences about the median of the typical difference. J Mod Appl Stat Met. 17:1.

Wilcox RR, Keselman HJ. 2003. Modern robust data analysis methods: measures of central tendency. Psychol Methods. 8:254.

Wilcox RR, Keselman HJ. 2012. Modern regression methods that can substantially increase power and provide a more accurate understanding of associations. Eur J Personality. 26: 165–174.

Wilcox RR, Rousselet GA. 2018. A guide to robust statistical methods in neuroscience. Curr Protocols Neurosci. 82(1): 8–42.

Wilcox RR, Serang S. 2017. Hypothesis testing, p values, confidence intervals, measures of effect size, and bayesian methods in light of modern robust techniques. Educ Psychol Meas. 77(4):673–689.

Yanai J, Pick CG, Rogel-Fuchs Y, Zahalka EA. 1992. Alterations in hippocampal cholinergic receptors and hippocampal behaviors after early exposure to nicotine. Brain Res Bull. 29:363–368.

Yawn BP, Suman VJ, Jacobsen SJ. 1998. Maternal recall of distant pregnancy events. J Clin Epidemiol. 51(5):399–405.

Zahalka EA, Seidler FJ, Lappi SE, McCook EC, Yanai J, Slotkin TA. 1992. Deficits in development of central cholinergic pathways caused by fetal nicotine exposure: differential effects on choline acetyltransferase activity and [3H]hemicholinium-3 binding. Neurotoxicol Teratol. 14:375–382.

Zhu AH, Salminen LE, Thompson PM, Jahanshad N. 2019. The UK Biobank Data Parser: a tool with built in and customizable filters for brain studies. Rome, Italy: Organization for Human Brain Mapping. Rome, Italy, June 9–13, 2019.

[CDC] Centers for Disease Control and Prevention. Health Effects of Secondhand Smoke. January 11, 2017; https://www.cdc.gov/tobacco/data_statistics/fact_sheets/secondhand_smoke/health_effects/index.htm. Accessed November 1, 2018.

[CDC] Centers for Disease Control and Prevention. Children in the Home. February 8, 2018; https://www.cdc.gov/tobacco/basic_information/secondhand_smoke/children-home/index.htm. Accessed November 1, 2018.

[WHO] World Health Organization. 2018. WHO Global Report on Trends in Prevalence of Tobacco Smoking 2000-2025. 2nd edn. Geneva: World Health Organization.